

PAPER • OPEN ACCESS

Development of HTS Current Leads for the ITER Project

To cite this article: P Bauer *et al* 2020 *IOP Conf. Ser.: Mater. Sci. Eng.* **756** 012032

View the [article online](#) for updates and enhancements.



EXTENDED ABSTRACT DEADLINE: DECEMBER 18, 2020

239th ECS Meeting
with the 18th International Meeting on Chemical Sensors (IMCS)

May 30-June 3, 2021

SUBMIT NOW →

The banner features a red top section with white text, a blue middle section with white text and logos, and a red bottom section with white text. The background of the blue section contains faint icons related to science and technology.

Development of HTS Current Leads for the ITER Project

P Bauer^{1*}, A Ballarino³, A Devred³, K Ding², Y Dong², E Niu⁴, Q Du², CY Gung¹, Q Han², R Heller⁵, X Huang², T Ichihara⁶, S Lee¹, J Li², C Liu², Cl Liu², K Lu², N Mitchell¹, Y Song², T Spina³, Q Ran², T Taylor⁷, S Yamada⁸, Y Yang⁹, T Zhou¹

¹ITER Organization, CS 90 046, 13067 St. Paul Lez Durance Cedex, France

²Institute of Plasma Physics, 350 Shushanhu Rd., 230031 Hefei, Anhui, China

³CERN, Route de Meyrin, 1211 Geneva, Switzerland

⁴China Fusion Domestic Agency, 15 Fuxing Rd, 100862, Beijing, China

⁵Karlsruhe Institute of Technology, PO box 3640, 76021 Karlsruhe, Germany

⁶Fusac Technologies, Osaka, Japan

⁷AT Scientific LLC, Geneva, Switzerland

⁸National Institute of Fusion Science, 322-6 Oroshi-cho, Toki, 509-5292 Japan

⁹Institute of Cryogenics, Univ of Southampton, University Road, SO17 1BJ, UK

E-mail: pierre.bauer@iter.org

Abstract. The HTS current leads for the ITER project will be the largest ever operated, with unprecedented currents, up to 68 kA and voltages, up to 14 kV. According to the ITER agreement they will be provided in-kind by China. After an extensive development program at the Hefei Institute of Plasma Physics (ASIPP), the ITER current leads were designed and qualified. The following discusses the main highlights of this development, with particular emphasis on the description of the design of the different types of ITER current leads and their final qualification in dedicated cold tests in nominal conditions.

1. Introduction

The ITER project to demonstrate the feasibility of power generation by nuclear fusion technology, now under construction in the south of France, requires very large superconducting magnets for confinement and control of the burning plasma. These large coils - 18 Toroidal Field Coils (TFC), six Central Solenoid (CS) modules, six Poloidal Field Coils (PFC) and 18 Correction Coils (CC) – are supplied with 60 HTS current leads, ranging from very large (68 kA for the TF) to medium (10 kA for the CC), transferring up to 2.6 MA into and out of the cryogenic environment (table 1). The largest (TF-type) leads are over 3 m long and weigh 600 kg. The ITER current leads are mounted horizontally into the so-called Coil Terminal Boxes (CTB) of the feeders, of which they are one of the key components [ref 1].

* To whom any correspondence should be addressed.



Table 1. Nominal operation parameters of the three types of ITER HTS current leads.

Parameter	TF	PF/CS	CC
Number of pairs	9	12	9
Design/operational max DC current (kA)	68/68	55/52	10/10
Operational max voltage/fault voltage to ground (kV)	7/19	14/29	0.3/3
Nominal operating temperature GHe supply to heat exchanger (K)		50	
Nominal operating pressure GHe supply to heat exchanger (MPa)		0.4	
Nominal operating temperature room temperature terminal (K)		~300	
Nominal operating temperature HTS top/warm end (K)		65	
Operating temperature HTS bottom/cold end (and LTS section) (K)		<7	
Maximum ramp-rate during pulse (kA/s)	-	20	10

Following CERN's successful development of HTS current leads for the LHC [ref 2, 3], ITER also launched R&D for HTS leads. Among the trials was the 70 kA "demonstrator", built by Germany's KIT and tested successfully at 70 kA in 2004 [ref 4-8]. Key technical design choices from the demonstrator survived into the final design, such as the counter-flow cooling of the resistive section with 50 K¹ helium gas from an intermediate cooling stage of the cryo-plant and the conduction cooling of the HTS section from the cold end. In 2004 the decision was made that the Chinese ITER partner supplies these HTS leads. ASIPP, which had recently completed the commissioning of the 16.5 kA HTS leads for the EAST Tokamak [ref 9], soon launched the manufacturing of several pre-prototypes for ITER [ref 10-17]. A 70 kA pre-prototype ("trial lead") was tested at up to 100 kA in December 2008 using the EAST power and cryogenic infrastructure, followed by a 52 kA PF-type lead and a 10 kA CC-type lead. These pre-prototype leads explored different resistive Heat eXchanger (HX) designs and jointing technologies. The final HTS shunt design incorporates many features of the ASIPP trial leads. The main technological design choices were finally fixed end of 2010. CERN's HX design was adopted, as well as its application of e-beam welding for precision and low heat input technique for joining the different lead sub-sections – HX, terminal and shunt [ref 3]. Generally, the ITER project chose to employ proven techniques and designs to minimize technical risk. The final design was jointly developed by ASIPP and ITER, under guidance from the HTS working group, a panel of experts. The following describes this development.

2. ITER Current Lead Design

The details of the design of the ITER HTS current leads can be found in [ref 19]. The main operational parameters are listed in table 1. As shown in figure 1 the ITER HTS current leads are assembled from: -1- the HTS shunt / LTS-linker and joint assembly, -2- the resistive Cu Heat eXchanger (HX), and -3- the Room Temperature (RT) terminal block.

The HTS-shunt, LTS linker and joint assembly is the component containing the superconductor, HTS and LTS. The complexity of this assembly comes from the multiple electrical splices - from the HX Cu to the HTS and from the HTS to the LTS. Located at the far end of the ITER feeders, the leads operate in a much lower magnetic field than the coils, such that the LTS linker is essentially a one meter piece of feeder cable in conduit (CIC) NbTi busbar [ref 20], terminated in a standard "Twin-Box" (TB) type joint [ref 21]. The HTS material is BiSCCO2223 (or Bi2223) tape with a specially alloyed Ag matrix containing 3 at% of Au to reduce the matrix thermal conductivity.

The resistive HX is machined from thick Cu stock, to form a central axial conductor with radial cooling fins. It is inserted into a thin-walled steel jacket, with very tight tolerance to limit bypass gas flow. The zigzag flow of GHe cooling is obtained by clipping the radial fins on alternating sides, maximizing the heat exchange surface. Its design is based on extensive modelling [ref 22]. Independent verifications with simplified models were also conducted [ref 23].

The RT terminal is designed for low current density, also in the contacts to the room temperature

¹ As shown in [ref 18] the ITER leads are operated close to the optimum cost with GHe injected at 50 K, implying a temperature of the HTS warm (top) end of 65 K.

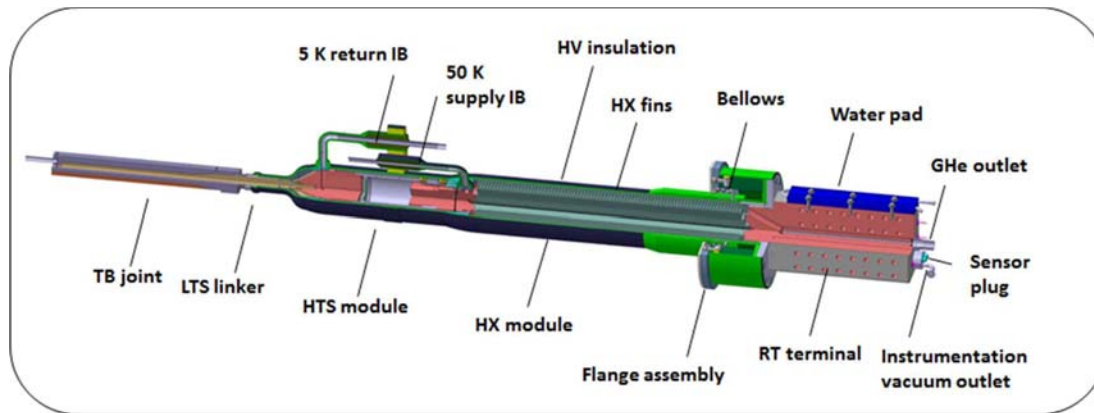


Figure 1. ITER HTS current lead design (TF-type).

busbar system. The HV insulation is designed to resist 30 kV with a large safety factor ($\sim 3-4$). It is made of a number of layers of polyimide combined with prepreg fiberglass sheets, adding up to six mm as described in [ref 24].

3. Qualification

The general methodology for the qualification of ASIPP and its two main sub-suppliers Juneng and Keye is discussed in [ref 25]. The complete supply chain had to be qualified, from material procurement, through targeted trials of critical manufacturing steps to the fabrication of technology mock-ups, and finally prototype leads of each type (PF, TF and CC).

First, all materials used require certification according to the applicable codes. The stainless steel is to conform to AISI 316L (level 3.1 certification according to EN 10204). OFE C10200 Cu must conform to standard ASTM B152 with an additional specification for the RRR value (40-200). Rigorous test schedules apply to the HTS tape (supplied by SEI-Japan and Innovia-China), including a minimum critical current I_c of 100 A @ 77 K in self-field (at 1 $\mu\text{V}/\text{cm}$ according to IEC 61788-3) and many more parameters. Continuous I_c and geometrical measurements are performed for the entire tape length. The insulation system is qualified for low void fraction ($<2\%$), minimum laminate shear strength (>50 MPa) and minimum ultimate tensile strength (500 MPa @ 0° , 200 MPa @ 90° to fiber), all after thermal cycling ([ref 26, 27]). With hundreds of box-type joints inside the ITER feeder system, the box joints were separately qualified in the framework of the feeder qualification. Further details of this are reported in [ref 21]. A major related effort was the development of suitable 316L steel – OFE Cu clad plates used for machining of the bimetal joint boxes [ref 28]. All the TIG welds were qualified according to EN ISO 15614-1:2004 (acceptance levels ISO5817 level B), including the additional requirement of five thermal cycles to liquid nitrogen (LN2) temperature. The brazing of the two major brazed subassemblies, HTS shunt and RT terminal, were qualified according to EN 13134:2000, with full-scale mock-ups, which were assessed through visual inspection (EN970), leak tested after 5 thermal shocks and destructively evaluated (metallography and tensile test according to ASME section IX). Imperfections were within the limits set by ISO 13919-1 level B. In the tensile test, failure occurred, as expected, in the copper (at ~ 180 MPa), not in the braze joint. Electron-Beam Welding (EBW) was qualified according to EN ISO 15614-11:2004. A special mock-up was made to develop the welding procedure. In addition to the ISO 13919-1 level B acceptance requirement, special requirements were also defined in this case including vacuum leak tests after thermal shocks and the evaluation of the length of the heat affected zone. The mock-up was also destructively tested to verify the quality and strength of the weld.

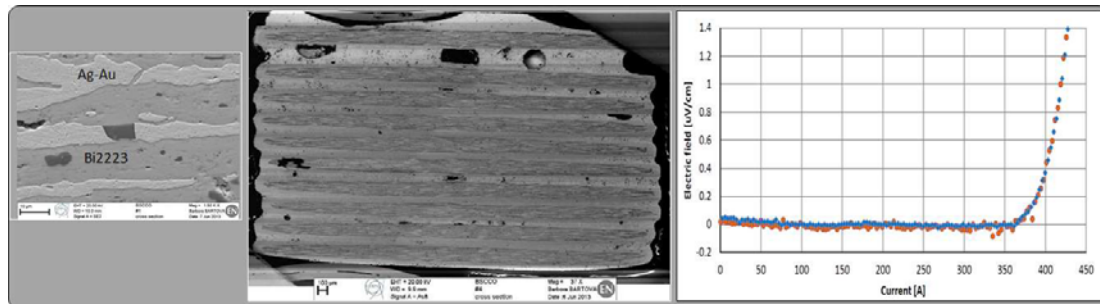


Figure 2. Left: micrograph of Innovia Bi-2223 tape, Middle: stack made by CERN from Innovia tape, Right: critical current measurement of two 5-stacks (CC-type) in self-field @ 77 K.

3.1 Technological Mock-ups

Technological mock-ups of different critical current lead subassemblies were built and tested for the different types of current leads by the respective suppliers [ref 29, 30], discussed in further detail below.

To qualify the stack-shunt soldering joints a 1/30 sample of a TF type shunt module was manufactured and tested. It consisted of three Bi-2223 HTS stacks soldered to a Cu-steel brazed plate, with a LTS sub-cable soldered into it. A major goal of this effort was to measure the joint resistance. Tape samples were also investigated at CERN and made into stacks (figure 2). Porosity found in the Ag-Au matrix of earlier tapes from Innovia were not found in subsequent samples.

The current lead sub-components requiring the most complex assembly is the low temperature end of the lead, which includes the joint box and the LTS section with several soldered electrical contacts. The most critical step is the soldering process between the LTS sub-cables and the shunt (figure 3). A specification for the electrical resistance must be met, requiring 100% wetting by solder of the bare strands, a tight fit between sub-cable and hole and complete filling of voids with solder. A resistance < 1 n Ω (for TF type lead) was found as required. After reverse plating, the other (joint box side) end was assembled into the joint-box together with a 0.3 mm Sn63Pb37 solder foil to improve the electrical contact to the Cu-sole. Microscopic, x-ray and mechanical examination of the mock-up joints demonstrated good bonding (peeling tests).

Following an early HX mock-up made at CERN to demonstrate the general feasibility and manufacturing technology, full size HX mock-ups of the TF and CC types were manufactured at Juneng and Keye. The tight H7g6 manufacturing tolerances between the core and honed tube were verified with coordinate measurement machine measurements of the HX core straightness (< 0.07 mm) and OD (< 0.03 mm tolerance) and with a feeler gage inserted into the honed tube with a special tooling. The HX mock-ups were submitted to a series of pressure drop tests with GN2 (nitrogen gas) and GHe at room temperature to establish a set of reference data for the future prototyping and series manufacturing. Due to their importance the measurements were performed at ASIPP and then repeated at CERN. The comparison of the experimental data to the model also helped the calibration of the HX model, as discussed in [ref 31]. A special measurement was performed on the TF HX mock-up in which capillaries were inserted along the HX to measure the pressure drop along four equally long sections. As expected the pressure drops of the four sections agreed, except for a slight increase from upstream to downstream resulting from the inlet pressure (into the specific segment), which is smaller for each segment as a result of the pressure drop in the previous segment(s). Finally X-ray tomography was used at CERN to verify that there were no bent fins or other defects in the HX honed tube assembly, which could not be detected by the pressure drop method (none was found).

Stringent qualification requirements were defined for the insulation system, as discussed above. To these are added particular requirements for the resin curing temperature ($\leq 80^\circ\text{C}$) and for the maximum boron content (zero, to prevent nuclear activation). The test requirements also include partial discharge



Figure 3. Preparing the sub-cables (TF-type): Left: chemical Ni removal, Middle: pre-tinning, Right: soldering into the shunt blind holes.

and Paschen testing. The development of a 30 kV class, combined polyimide / impregnated glass fiber (“GK”) system required significant R&D (it was completed only at the very end of the lead development). The ASIPP efforts are discussed in [ref 32]. Partial discharge levels found in the mock-up tests are consistent with those of small, flat samples for which the void fraction was measured to be within specification. Extensive R&D was also conducted for the insulated heaters and room temperature Insulating Breaks (IB) for the RT terminals [ref 33, 34], special developments for the HTS leads.

3.2 Prototypes

A pair of each type of current lead was tested as the final step of the qualification process. More details on CC, PF and TF prototype manufacture and testing are discussed in: [ref 35, 36, 37, 38 for CC] and [ref 39, PF] and [ref 40, TF]. The test data are summarized in table 2. The tests were conducted in a new ASIPP test facility including a 900 W @ 4.5 K He plant and a 80 kA power supply system as described in [ref 41,42]. It also includes a control and interlock system supplied by ITER. Figure 4 shows the TF lead prototypes mounted in series inside a prototype CTB, shorted by a removable superconducting U-bend with clamped TB joints. The leads were fully instrumented with voltage taps for quench detection and measurement of the different joint resistances and with temperature sensors in key locations. The 50 K and 5 K hydraulic circuits were instrumented with pressure gages and temperature sensors at the inlet/outlet and flow-meters at the outlet. The two HX were supplied in parallel with 50 K GHe with the flow being regulated with a valve downstream of the 300 K GHe exhaust of each lead. At the 5 K ends the leads were supplied with 5 K SHe, entering through the TB joint of one lead, then flowing through the CIC- type U-bend and exiting after the LTS linker of the other lead. The SHe could be heated to room temperature in a large heat exchanger downstream of the CTB, to allow a precise flow measurement with a flow-controller. As will be done in ITER, large water-cooled Al busbars transferred the currents from the power supply to the HTS current lead test-station, where air-cooled flexibles connected them to the current lead terminals.

Steady state tests were performed at different currents (80, 90, 100 and 110% of the nominal). Figure 5 shows the performance parameters of the HX (voltage drop, steady state mass-flow) for the different currents. In the case of the TF prototypes the agreement of these parameters with the CERN model is good, as can be seen from the figure. Also for the CC mass-flow rates are predicted well by the model from [ref 38]. The joint resistances found during steady operation were below specification (table 2).

Following the steady state operation test, the HTS was quenched by a LOFA (Loss Of Flow Acc) event, i.e. by stopping the 50 K GHe cooling flow while keeping the full current. The quench is defined



Figure 4. TF current leads installation in the test cryostat.

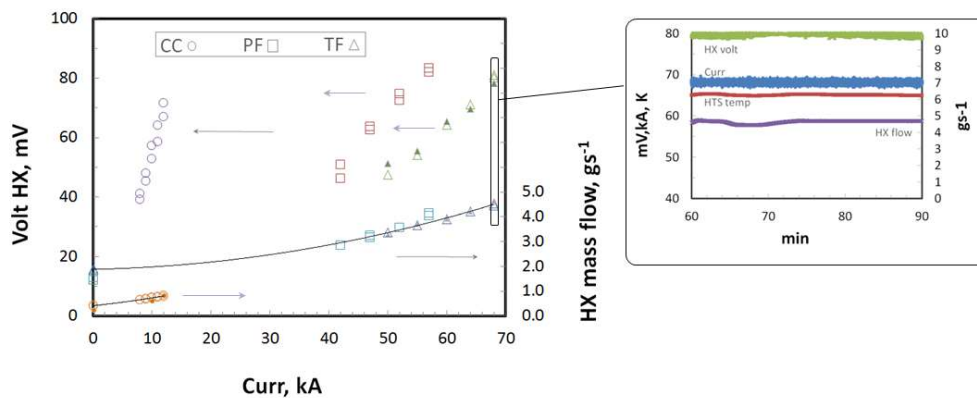


Figure 5. Prototype steady state HX voltage and mass-flow rate compared to model (full markers - CERN model for TF, [ref 38] model for CC). Insert: steady state in the TF prototype at 68 kA.

as occurring when the HTS voltage exceeds 2 mV. The temperature at the top of the HTS first rises slowly to ~ 90 K when the quench occurs and the temperature rises fast with the current being switched off when the hot-spot reaches 200 K. The hot-spot is located a bit below the top (warm) end of the HTS, where the shunt steel cross-section underneath the HTS is reduced and the heat diffusion and current sharing therefore less effective. Thermal-cycling and multiple LOFA quenches did not impact on the performance of the leads.

The heat conduction of the current lead was measured calorimetrically at zero current. After stabilizing the 5 K SHe cooling of the LTS loop (including the U-bend) for a given HTS top temperature in steady state (65, 80 or 100 K), the heat load was computed from the enthalpy difference (obtained from SHe temperature and pressure at the inlet/outlet) multiplied by the mass-flow. This technique applies to the entire 5 K loop and does not differentiate between the two leads (the total number is therefore divided by 2 in table 2). To check that the heat conduction from the two leads was balanced, the heat load was also derived from the shunt temperature measurements. This method consists of plotting the recorded temperature readings along the shunt and tuning the conduction heat load in the calculated temperature profile until it matches. Although this method was less precise (with only three temperature measurement points), its consistency with the heat load value obtained from halving the 5 K circuit enthalpy validated the calorimetric approach (and the material properties models).

A key parameter, which was modified after completion of the current lead design, is the 50 K GHe supply condition for the resistive heat exchanger. Originally defined as 50 K (± 2 K), it was changed to a looser 40 K - 52 K. Special studies were performed to explore the impact of lower inlet temperatures (and pressures) for the HX operation. It emerged from this study that, provided the difference between GHe inlet temperature and the HTS top temperature remains 15 K, there is no difference in HX operation between 50 K and 40 K GHe supply temperature. The mass-flow is close to nominal and the lead operates stably. However, if this temperature interval is allowed to increase, the HX becomes unstable. For example, the HX voltage cannot stabilize for the condition $T_{\text{He,in}} = 40$ K and $T_{\text{HTS-top}} = 65$ K, as the mass-flow for this temperature at the cold end of the HX is insufficient to cool its warm end. This result implies that operation in ITER with “looser” temperature tolerances at the inlet will require also changing the $T_{\text{HTS-top}}$ set-points for controlling mass-flow (e.g. for 40 K supply $T_{\text{HTS-top}} = 55$ K). While the effect of lower inlet temperatures can be managed with an improved control algorithm, the effect of inlet pressure is more serious. The pressure drop in the HX increases when the inlet pressure is reduced, leading to a choking effect, i.e. at lower supply pressure the mass-flow through the HX is reduced, possibly leading to a thermal runaway. Lower pressure at the outlet also affects the electrical breakdown strength of the helium in the RTIBs. It is recommended that for operation the GHe supply pressure remains above ~ 3.8 bar (and below ~ 5 bar, as the safety valves for the current leads open at ~ 5.5 bar).

While the ITER TF type current leads operate in steady state, the PF-type and CC-type leads operate

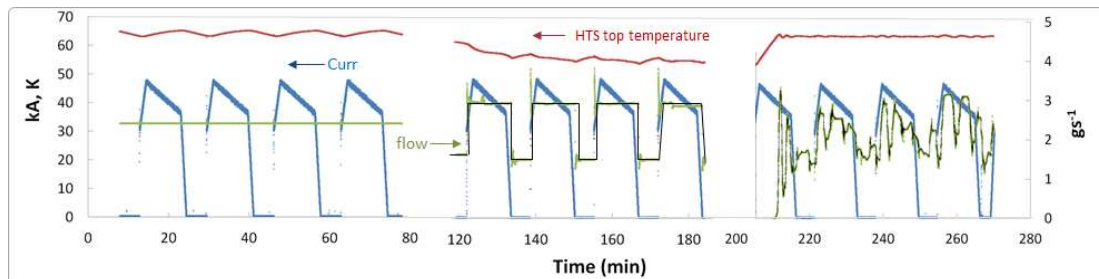


Figure 6. Three different flow control modes in the PF type current lead 1. Left: single flow (manual), Middle: "two-flow" (manual), Right: PID control. Temperature profiles shown are for steady state.

in pulsed mode. The prototypes were therefore charged with a typical ITER pulse current pattern to investigate their response. For the PF-type leads, the simulated pulse was rectangular with fast ramps (figure 6). Three different current lead control modes were explored. The simplest consisted of applying a constant flow in the HX calculated from the average current in the pulse (note that the zero current flow rate is the "stand-by" flow rate and not zero). The so-called "two-flow" mode oscillates between the stand-by flow at zero-current and the max-flow at the pulse maximum current. Finally a PID control mode was also tested, with the PID parameters set according to the results of open loop response tests. In all three modes the HTS top temperature is reasonably well controlled. There are, however, qualitative differences: the GHe control valve (located at the 300 K exhaust) works much harder in the automatic control mode. It shall also be considered to correlate the required flow-rate with the square of the current.

The HX pressure drops were usually obtained from the difference between the inlet and outlet absolute pressure measurements. This is not as accurate as the use of properly chosen differential pressure gages, but was good enough, at least for the TF and PF-type leads, which have a significant p-drop in nominal conditions (~1 bar). As shown in figure 5 they also compare well to the prediction by the CERN model. The pressure drop in the CC leads, however, is very small, only a few kPa and not measurable with the absolute gauges used. In this case pressure drop measurements were conducted with GHe at room temperature and compared to those obtained in similar conditions in the CC HX mock-up. These comparisons showed no evidence of by-pass flow, further corroborating the fact that geometrical data obtained on the HX cores and honed tubes during manufacturing were within specifications. One of the TF and CC prototypes were subjected to a full suite of HV measurements, including hi-pot to 30 kV, Partial Discharge (PD) to 10 kV and Paschen tests (the other leads did not have the finally developed insulation scheme). These leads passed these tests, see table 2.

Table 2. Test results for the ITER prototype HTS current leads.

Qualification Parameter	TF I	TF II	PF I	PF II	CC I	CC II
Leak rate 50 K loop at test pressure (10^{-9} Pa-m ³ /s)	0.49	0.49	0.12	0.25	0.4	0.4
Leak rate 5 K loop at test pressure (10^{-9} Pa-m ³ /s)	0.83	0.83	0.27	0.27	0.28	0.28
Cold end heat load with HTS top at 65 K (W)	20/2	20/2	20/2	20/2	2*	N/A
Pressure drop in HX section at max DC curr (MPa)	0.13	0.125	0.066	0.065	0.005	0.007
50 K GHe steady state flow-rate at max DC curr (g/s)	4.6	4.7	3.6	3.6	0.7	0.6
50 K GHe steady state flow-rate at zero curr** (g/s)	1.9	1.9	1.55	1.45	0.3	0.3
Nominal operating voltage HX at max DC curr (mV)	77	76	74	73	60	63
Temp margin (2 mV crit) in ITER condition (K)***	27	27	31	31	30	30
LOFA time at max DC operation current (2mV) (s)***	480	480	690	690	1020	1020
HTS over-heating time (2 mV criterion) (s)***	18	15	37	27	28	26
RT terminal and interface BB contact resistance (nΩ)	400	200	200	100	N/A	N/A
HX to HTS joint resistance (nΩ)	5.5	5.4	5.1	4.8	15.8	9.4
HTS to LTS joint resistance (nΩ)	0.1	0.4	0.2	0.3	0.4	0.4
HTS-CL to feeder busbar TB joint resistance (nΩ)	0.5	0.5	0.6	0.6	0.4	0.2
Resistance to ground in hi-pot test (GΩ)	3.3	N/A	30	N/A	50	4.5
Equivalent charge during PD test (nC)	5.0	N/A	2.5	N/A	N/A	0.1
Paschen test (@ 15 kV)	pass	N/A	N/A	N/A	N/A	pass

* obtained with the temperature profile method only; ** with 65 K at the HTS top; ***does not take into account the external stray field of ITER;

4. Summary

HTS current leads are one of the enabling technologies for fusion Tokamaks, as they reduce the input power requirement for plant operation. At 68 kA the ITER TF type HTS current leads will be the largest ever operated. The considerable effort to design them and qualify their manufacturing is described here.

5. Disclaimer

The views and opinions expressed herein do not necessarily reflect those of the ITER organization.

6. References

- [1] Bauer P et al, 2012 *IEEE Trans Appl SC* **22/3** 4800504
- [2] Taylor T, 1999 *IEEE Trans Appl SC* **9** 412
- [3] Ballarino A, 2002 *Physica C* **372-376** 1413
- [4] Heller R et al, 2004 *IEEE Trans Appl SC* **14/2** 1774
- [5] Heller R et al, 2005 *IEEE Trans Appl SC* **15/2** 1496
- [6] Heller R, Fietz WH, Lietzow R, Tanna VL, Vostner A, Wesche R, Zahn GR, 2006 *IEEE Trans Appl SC* **16/2** 823
- [7] Fietz W, Heller R, Lietzow R, Tanna VL, Zahn G, Wesche R, Salpietro E, Vostner A, 2005 *21st IEEE/NPS Symposium on Fusion Engineering*
- [8] Heller R, 2009 *IEEE Trans Appl SC* **19/3** 1504
- [9] Bi Y, Chen X, Ma D, Liu X, Wu S, Li J, 2005 *Proceedings of ICEC 20* 681
- [10] Bauer P et al, 2009 *IEEE Trans Appl SC* **19/3** 1500
- [11] Bi Y et al, 2010 *IEEE Trans Appl SC* **20/3** 1718
- [12] Ding K, Bi Y, Yu J, Zhou T, Liu CL, Lin X, Shen G, Song Y, 2010 *IEEE Trans Appl SC* **20/3** 1729
- [13] Huang X, Bi Y, Cheng Y, Lu L, Wang C, Shen G, Song Y, 2010 *IEEE Trans Appl SC* **20/3** 1722
- [14] Bauer P et al, 2011 *IEEE Trans Appl SC* **21/3** 1074
- [15] Liu C et al, 2012 *IEEE Trans Appl SC* **22/3** 4800204
- [16] Ding K et al, 2012 *Physics Procedia* **36** 931
- [17] Zhou T, Ding K, Liu CL, Bi Y, Song Y, 2015 *IEEE Trans Appl SC* **25/2** 4802704
- [18] Wesche R, Heller R, Bruzzone P, Fietz WH, Lietzow R, Vostner A, 2007 *Fusion Eng and Design* **82** 1385
- [19] Taylor T, 2012 *IEEE Trans Appl SC* **22/3** 4800304
- [20] Calvi M, Bauer P, Bessette D, Cau F, Marinucci C, Bruzzone PL, 2010 *IEEE Trans Appl SC* Vol **20** No 3 p 407
- [21] Ilin Y et al, 2016 *IEEE Trans Appl SC* **26/4** 4800905
- [22] Sitko M, Bordini B, Ballarino A, Bauer P, Devred A, 2013 *IEEE Trans Appl SC* **23/3** 4900805
- [23] Rizzo E, Heller R, Savoldi Richard L, Zanino R, 2012 *IEEE Trans Appl SC* **22/3** 4801104
- [24] Knaster J, Rajainmaki H, Evans D, Losasso M, 2013 *IEEE Trans Appl SC* **23/3** 3800505
- [25] Bauer P et al, 2013 *IEEE Trans Appl SC* **23/3** 4801104
- [26] Clayton N, Crouchen M, Devred A, Evans D, Gung CY, Lathwell I, 2017 *Cryogenics* **83** 64
- [27] Huang X et al, 2017 *Fusion Eng and Design* **114** 13
- [28] Langeslag S A E, Sgobba S, Libeyre P, Gung C Y, 2015 *Physics Procedia* **67** 1036
- [29] Zhou T, Lu K, Ran Q, Ding K, Feng HS, Wu H, Liu CL, Song Y, Niu E, Bauer P, 2014 *IEEE Trans Appl SC* **24/3** 4801205
- [30] Zhou T, Lu K, Ran Q, Ding K, Feng HS, Wu H, Liu CL, Song Y, Niu E, Bauer P, Devred A, 2015 *Fusion Eng and Design* **96-97** 388
- [31] Bauer P, Ballarino A, Bordini B, Devred A, Ding K, Niu E, Sitko M, Taylor T, Yang Y, Zhou T, 2015 *IOP Conf. Series: Materials Science and Engineering* **101** 012119
- [32] Huang X et al, 2019 *Fusion Eng and Design*, **146** 955
- [33] Fietz WH, Fink S, Kraft G, Scheller H, Urbach E, Zwecker V, 2013 *IEEE Trans Appl SC* **23/3** 4200604
- [34] Pan W, Bauer P, Carrillo D, Journeaux J, Zhu Y, Wu C, Cao Y, Chen X, 2019 *Fusion Eng and Design* **143** 154
- [35] Zhou T et al, 2016 *IEEE Trans Appl SC* **26/6** 4802505
- [36] Zhou T et al, 2015 *2015 IEEE 26th Symposium on Fusion Engineering (SOFE)*
- [37] Ding K et al, 2016 *IEEE Trans Appl SC* **26/4** 4803404
- [38] Zappatore A, Heller R, Bauer P, Savoldi L, Zanino R, 2016 *Cryogenics* **80/3** 325
- [39] Liu C, Ding K, Zhou T, Du Q, Dong Y, Han Q, Lu K, Song Y, Niu E, Bauer P, 2018 *IEEE Trans Plasma Sci* **46/9** 3219
- [40] Ding K et al, 2019 *IEEE Trans Appl SC* **29/5** 4802605
- [41] Ding K, Liu CL, Bi Y, Feng HS, Du Q, Zhou T, Lu K, Song Y, Xu L, 2016 *IEEE Trans Appl SC* **26/3** 9500604
- [42] Liu C, Ding K, Du Q, Dong Y, Wang J, Lu K, Song Y, Niu E, Bauer P, 2019 *IEEE Transactions on Plasma Sci* **47/1** 795